Article

A Computational Framework for Load-Constrained Human Squat Motion with Nonlinear Joint Modeling

Karol Nowak , Anna Szymczak-Graczyk , Aram Cornaggia , Tomasz Garbowski *

Posted Date: 25 March 2026

doi: 10.20944/preprints202603.1971.v1

Keywords: human squat biomechanics; joint moment capacity; plastic hinge; motion optimization; load-constrained human motion; multibody kinematics; nonlinear joint mechanics

 doi:10.20944/preprints202603.1971.v1

Article

A Computational Framework for Load-Constrained Human Squat Motion with Nonlinear Joint Modeling

Karol Nowak [1], Anna Szymczak-Graczyk [2], Aram Cornaggia [3] and Tomasz Garbowski [4,*]

[1] Faculty of Education Studies, Kazimiera Milanowska College of Education and Therapy, 61-473 Poznan, Poland

[2] Faculty of Environmental and Mechanical Engineering, Poznan University of Life Sciences, 60-637 Poznan, Poland

[3] Department of Engineering and Applied Sciences, Universit`a degli studi di Bergamo, 24044 Dalmine, BG, Italy

[4] University Center for Ecomaterials, Poznan University of Life Sciences, 60-637 Poznan, Poland

* Correspondence: tomasz.garbowski@up.poznan.pl

Abstract

Human squat motion is commonly analyzed using inverse dynamics, where joint moments are computed from experimentally measured kinematics. Such analyses typically assume that the observed motion is mechanically feasible and do not explicitly account for limitations of joint moment capacity. In this study, a computational framework is proposed for the load-constrained reconstruction of squat motion that integrates kinematic motion generation with a mechanical model of moment-limited joints. The human body is represented as a multi-segment system consisting of feet, shanks, thighs, pelvis, and torso. Joint behavior is modeled using nonlinear rotational springs with bounded moment capacity, allowing elastic response followed by progressive softening when critical moments are approached. A reference squat trajectory is first generated kinematically, after which a constrained optimization problem is solved at each motion frame to obtain a mechanically admissible posture under external loading. The objective function combines trajectory tracking with joint energy contributions, while gravitational loading from a barbell applied at the shoulders introduces external work. The formulation enables automatic correction of the reference motion when joint moment limits are exceeded, resulting in mechanically admissible squat postures. Numerical examples illustrate the evolution of pelvis trajectory, torso inclination, lower-limb segment angles, and reconstructed body configurations throughout the squat cycle.

Keywords: human squat biomechanics; joint moment capacity; plastic hinge; motion optimization; load-constrained human motion; multibody kinematics; nonlinear joint mechanics

1. Introduction

The squat is one of the most widely used multi-joint resistance exercises in both athletic training and rehabilitation, and has therefore been extensively investigated in the biomechanical literature [1,2]. As a complex movement involving coordinated interaction of the lower limbs and torso, the squat requires simultaneous control of multiple joints and segments, allowing for a wide range of movement strategies depending on technique, load, and individual characteristics [3–5].

Variations in squat technique have been shown to significantly influence kinematics, kinetics, and muscle activation patterns. In particular, stance width, bar position, and movement strategy affect joint angles and load distribution across the hip, knee, and ankle joints [6–8]. One of the most debated aspects of squat mechanics is the anterior displacement of the knee relative to the toes. It is commonly suggested that limiting forward knee travel reduces knee joint loading while increasing the contribution of the hip extensors [9]. Experimental studies have confirmed that restricting knee

 doi:10.20944/preprints202603.1971.v1

displacement leads to a decrease in knee torque accompanied by a substantial increase in hip torque and modifications in torso inclination [10].

These findings have contributed to the development of distinct squat techniques, including the traditional squat, powerlifting squat, and box squat, which differ in stance width, hip displacement strategy, and torso orientation [2,11]. The traditional squat is typically characterized by a narrower stance and greater anterior knee displacement, resulting in forward movement of the system center of mass (COM). In contrast, the powerlifting squat and box squat emphasize posterior displacement of the hips and a more vertical shin position, often producing a posterior shift of the COM and altered joint loading patterns [2].

Previous experimental studies have demonstrated that such variations in technique lead to significant differences in joint kinematics and kinetics. Wide-stance squats are associated with increased hip extension moments and reduced ankle moments, whereas modifications such as the use of a box alter force-time characteristics and reduce the contribution of the stretch–shortening cycle [12–14]. Additionally, differences in femur rotation, hip abduction, and coordination patterns have been linked to variations in muscle activation and joint loading, which may influence both performance and injury risk [15–17].

The mechanical consequences of squat technique have also been analyzed in relation to joint loading and injury mechanisms. It has been suggested that combined hip adduction and internal rotation may increase stress at the knee joint and contribute to injuries such as anterior cruciate ligament strain or patellofemoral pain syndrome [18,19]. Furthermore, accurate quantification of joint kinematics and center of mass motion plays a key role in biomechanical analysis, with established modeling approaches providing the basis for inverse dynamics calculations [20,21].

In addition to internal joint mechanics, the external mechanical stimulus of the squat has been widely studied through variables such as force, velocity, power, and rate of force development (RFD). These parameters are commonly used to assess training effectiveness and to optimize loading conditions in resistance exercises [22–24]. In particular, the ability to generate high power and RFD has been associated with improved athletic performance, although the relationship between training methods and long-term adaptations remains complex [25]. The role of musculotendinous stiffness and its interaction with eccentric–concentric transitions has also been highlighted as an important factor influencing force production and movement efficiency [26].

Experimental studies comparing different squat techniques have further demonstrated that variations in execution can significantly affect peak power, ground reaction forces, and movement velocity, reinforcing the importance of technique selection in strength training practice [27,28]. Moreover, observational studies of elite athletes indicate that training strategies and technique adaptations are influenced by both performance goals and individual biomechanical constraints [29]. These findings are also reflected in broader training guidelines, which emphasize the importance of progressive overload and individualized exercise prescription [30].

Despite the substantial body of experimental work, most existing studies rely on inverse dynamics approaches, in which joint moments are computed from measured kinematics and external forces. While these methods provide valuable insight into the mechanical consequences of observed motion, they do not explicitly account for limitations in joint moment capacity and therefore do not address whether a given movement pattern is mechanically admissible.

From a mechanics perspective, human motion can be interpreted as the result of constraints imposed by geometry, external loading, and internal strength limits. In this context, joint moment capacity may act as a governing constraint that shapes movement strategies, particularly under high external loads. However, this aspect has received limited attention in current biomechanical modeling of the squat.

The aim of the present study is therefore to develop a computational framework for reconstructing squat motion under external loading while explicitly accounting for joint moment capacity. The proposed approach integrates kinematic trajectory generation with a nonlinear mechanical model of moment-limited joints and a constrained optimization procedure, allowing the

 doi:10.20944/preprints202603.1971.v1

motion to adapt to mechanical limitations rather than being prescribed a priori. This formulation provides a complementary perspective to classical inverse dynamics and enables systematic investigation of load-dependent adaptations in squat technique.

2. Materials and Methods

2.1 Overview of the Computational Framework

The objective of the proposed framework is to compute mechanically admissible squat postures under external loading while respecting the strength limits of human joints. The approach combines a kinematic motion generator with a nonlinear mechanical solver that corrects the reference motion when joint moment capacities are exceeded.

The overall procedure consists of three main stages: (1) generation of a reference squat trajectory using a kinematic model, (2) reconstruction of body segment positions using inverse kinematics, (3) mechanical correction of the posture through optimization with nonlinear joint constraints. The computational workflow is illustrated schematically in Figure 1.

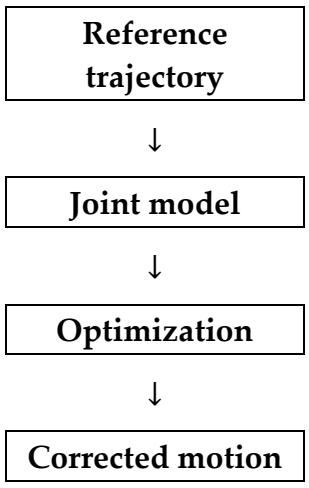

Figure 1. Schematic representation of the proposed computational workflow. The framework combines reference trajectory generation, geometric reconstruction of the body, nonlinear joint modeling, and constrained optimization to obtain mechanically admissible squat motion.

The key idea of the method is that the reference trajectory does not necessarily represent a mechanically feasible posture under external loading. Instead, the final posture is obtained by solving a constrained optimization problem in which the body configuration adapts to both external forces and joint moment limits.

2.2 Geometric Model of the Body

The human body is represented as a multi-segment system consisting of rigid links corresponding to the feet, shanks, thighs, pelvis, and torso. The model distinguishes between the left and right lower limbs, while the pelvis and shoulders are represented as horizontal connecting segments.

A global Cartesian coordinate system $(X, Y, Z)$is used, where the X-axis denotes the anterior–posterior direction, the Y-axis the lateral direction, and the Z-axis the vertical direction.

The pelvis center is defined by the coordinates

$$\mathbf{p}_p = \begin{bmatrix} x_p \\ 0 \\ z_p \end{bmatrix}, \tag{1}$$

 doi:10.20944/preprints202603.1971.v1

and its orientation is described by two rotations: a yaw rotation about the vertical axis and a tilt rotation about the sagittal axis.

The corresponding rotation matrix is

$$\mathbf{R}_p = \mathbf{R}_z(\psi_p)\mathbf{R}_x(\phi_p), \tag{2}$$

where ψ_p denotes the pelvis yaw and ϕ_p the pelvis tilt.

The hip joint centers are obtained from the pelvis center and pelvis width b_p,

$$\mathbf{p}_{H_L} = \mathbf{p}_p + \frac{b_p}{2}\mathbf{e}_{y,p}, \quad \mathbf{p}_{H_R} = \mathbf{p}_p - \frac{b_p}{2}\mathbf{e}_{y,p}, \tag{3}$$

where $\mathbf{e}_{y,p}$is the transverse unit vector of the pelvis.

The ankle joints are assumed fixed in space during the squat motion,

$$\mathbf{p}_{A_L} = \mathbf{p}^0_{A_L}, \quad \mathbf{p}_{A_R} = \mathbf{p}^0_{A_R}. \tag{4}$$

2.3 Inverse Kinematics of the Lower Limbs

Each leg is reconstructed independently in a local sagittal plane defined by the foot orientation. Let L_s and L_f denote the lengths of the shank and thigh, respectively.

The knee position is obtained as the intersection of two circles defined by the segment lengths,

$$x_K^2 + z_K^2 = L_s^2, \tag{5}$$

$$(x_H - x_K)^2 + (z_H - z_K)^2 = L_f^2, \tag{6}$$

where (x_H, z_H) denote the hip coordinates expressed in the local leg plane.

The inverse kinematics solution exists provided that

$$|L_s - L_f| \leq \sqrt{x_H^2 + z_H^2} \leq L_s + L_f. \tag{7}$$

This formulation guarantees that the segment lengths remain constant and ensures geometric compatibility between the pelvis motion and the lower limbs.

2.4 Reference Squat Trajectory

A reference squat motion is generated using a parametric trajectory defined by a normalized motion parameter $s \in [0,1]$. The parameter $s = 0$ corresponds to the initial upright posture, while $s = 1$ represents the deepest squat position.

To ensure smooth motion, the profile function

$$f(s) = 3s^2 - 2s^3, \tag{8}$$

is used.

The reference pelvis motion is then defined as

$$x_p^{\text{ref}}(s) = x_{p,0} - \Delta x_p f(s), \tag{9}$$

$$z_p^{\text{ref}}(s) = z_{p,0} - \Delta z_p f(s), \tag{10}$$

while the rotations evolve according to

$$\psi_p^{\text{ref}}(s) = \psi_{\max} f(s), \tag{11}$$

$$\phi_p^{\text{ref}}(s) = \phi_{\max} f(s), \tag{12}$$

$$\theta_t^{\text{ref}}(s) = \theta_{t,\max} f(s), \tag{13}$$

where the parameters Δx_p, Δz_p, $\psi_{\max}$, $\phi_{\max}$, and $\theta_{t,\max}$ define the amplitude of the squat motion.

 doi:10.20944/preprints202603.1971.v1

2.5 Nonlinear Joint Model

The joints are represented using nonlinear rotational elements with bounded moment capacity. Let $\Delta\theta_j$ denote the deviation of a joint angle from its reference value,

$$\Delta\theta_j = \theta_j - \theta_j^{\text{ref}}. \tag{14}$$

The moment generated in joint j is described by the relation

$$M_j = M_{y,j}\tanh\left(\frac{k_j\Delta\theta_j}{M_{y,j}}\right), \tag{15}$$

where k_j is the rotational stiffness and $M_{y,j}$ is the maximum moment capacity.

This formulation approximates linear elastic behavior for small rotations while smoothly limiting the moment as the joint approaches its strength capacity.

The associated energy stored in the joint is obtained by integrating Eq. (15),

$$\Pi_j = \frac{M_{y,j}^2}{k_j}\ln\left(\cosh\left(\frac{k_j\Delta\theta_j}{M_{y,j}}\right)\right). \tag{16}$$

2.6 External Loading

The external load is represented by a barbell of mass m_b acting vertically at the shoulder joints. The total barbell weight is

$$W_b = m_b g, \tag{17}$$

where g is gravitational acceleration.

Assuming equal load distribution between the shoulders, the gravitational potential energy contribution becomes

$$\Pi_{ext} = \frac{1}{2}W_b z_{S_L} + \frac{1}{2}W_b z_{S_R}. \tag{18}$$

2.7 Optimization Problem

The mechanically admissible posture is obtained by minimizing the total energy functional

$$\Pi(\mathbf{q}) = \Pi_{\text{track}} + \Pi_{\text{joint}} + \Pi_{\text{ext}}, \tag{19}$$

where the tracking term penalizes deviations from the reference trajectory,

$$\Pi_{track} = \frac{1}{2}(\mathbf{q} - \mathbf{q}^{\text{ref}})^T\mathbf{K}_{\text{track}}(\mathbf{q} - \mathbf{q}^{\text{ref}}). \tag{20}$$

The optimization problem solved at each frame is therefore

$$\mathbf{q} = \arg\min_{\mathbf{q}} \Pi(\mathbf{q}), \tag{21}$$

subject to the geometric feasibility constraints of the lower limbs.

2.8 Numerical Implementation

The optimization problem is solved sequentially for each frame of the squat trajectory using a nonlinear constrained optimization algorithm. The solution obtained for the previous frame serves as the initial guess for the next frame, which improves convergence and ensures temporal continuity of the motion. The numerical procedure follows a continuation strategy along the motion parameter, allowing the solver to progressively adapt the configuration while maintaining geometric compatibility of the lower limbs.

After the corrected posture is determined, the joint moments are evaluated and compared with their respective capacities. If the moment in a given joint approaches the critical value, the joint stiffness is reduced in subsequent frames to represent progressive mechanical softening. This

 doi:10.20944/preprints202603.1971.v1

mechanism enables the model to capture the gradual redistribution of rotational demand between joints when local strength limits are approached.

The complete computational workflow, including the generation of the reference trajectory, reconstruction of body geometry, inverse kinematics of the lower limbs, nonlinear evaluation of joint moments, and sequential stiffness updates, is summarized in the form of detailed pseudocode in Appendix A. The presented algorithms clarify the interaction between the kinematic motion generator and the mechanical correction procedure used to obtain the final squat motion.

This frame-by-frame correction procedure produces a squat motion that satisfies both the kinematic constraints of the body segments and the mechanical limitations of the joints.

3. Results

The numerical results presented in this section illustrate the kinematic behavior of the proposed computational framework and demonstrate how the reconstructed squat motion evolves along the prescribed movement path. The results are organized to highlight four aspects of the analysis: the reference trajectory of the pelvis and torso, the evolution of three-dimensional body configurations, the angular histories of the main body segments, and the geometric consistency of the reconstructed motion assessed through left–right spacing, sagittal posture overlays, and trajectories of selected anatomical points.

The reference squat trajectory generated by the kinematic motion driver defines the intended movement of the pelvis and torso during the squat. Figure 2 presents the evolution of the pelvis center coordinates and the torso pitch angle along the normalized motion parameter s. The trajectory represents a typical squat pattern characterized by a gradual vertical descent of the pelvis combined with a posterior displacement and increasing torso inclination.

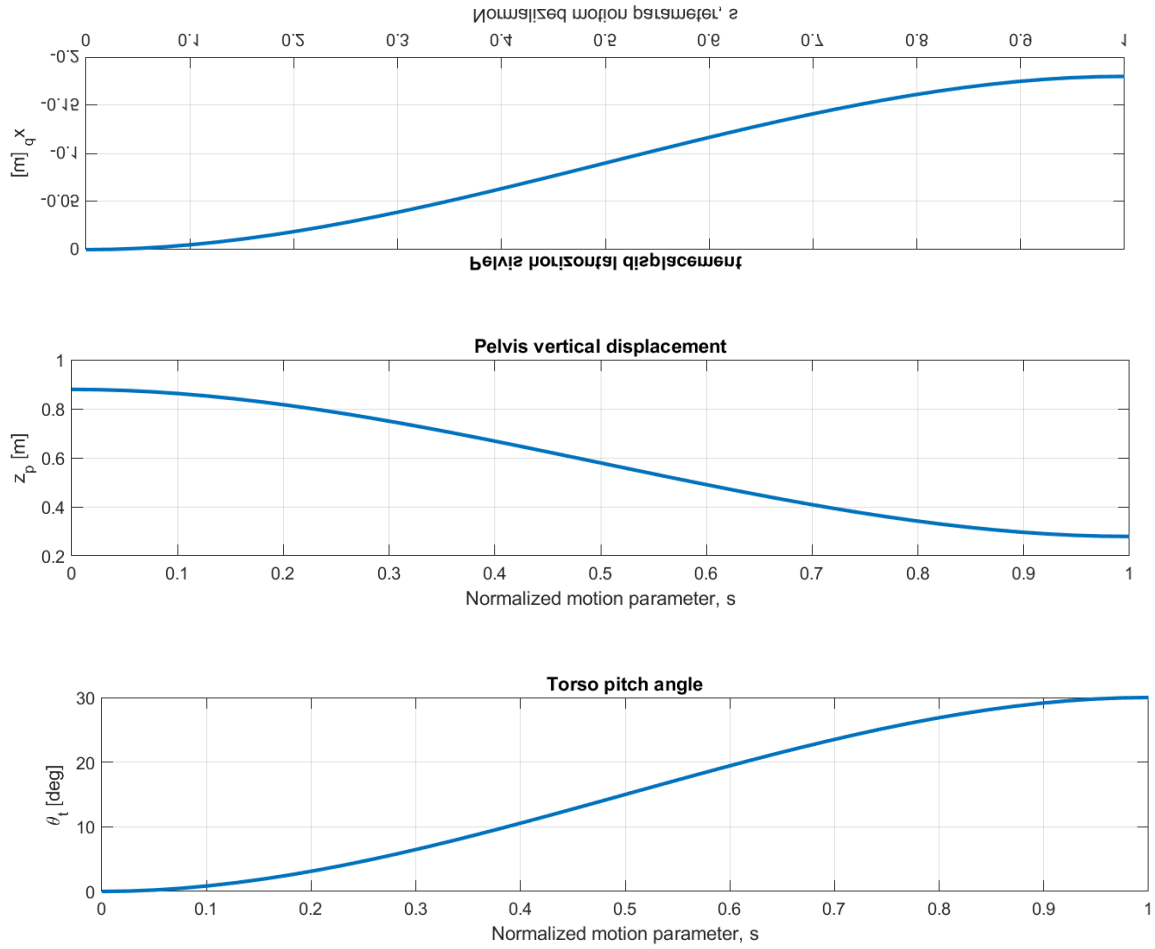

 doi:10.20944/preprints202603.1971.v1

Figure 2. Evolution of pelvis kinematics and torso orientation during the squat motion: (a) horizontal displacement of the pelvis center x_p, (b) vertical displacement of the pelvis center z_p, (c) torso pitch angle. All quantities are shown as functions of the normalized motion parameter s.

The generated trajectory provides the input configuration for the mechanical solver. However, because the reference motion is constructed purely kinematically, it does not necessarily satisfy the mechanical constraints imposed by joint moment capacity when external loads are applied. The role of the optimization procedure introduced in Section 2 is therefore to compute a mechanically admissible posture that remains close to the reference trajectory while respecting the nonlinear joint model.

Figure 3 presents selected three-dimensional body configurations at representative stages of the squat cycle. The reconstructed poses show the progressive descent of the pelvis, increasing flexion of the lower limbs, and gradual forward rotation of the torso as the motion parameter increases from the upright configuration to the deepest squat position. The sequence confirms that the adopted geometric reconstruction remains continuous and anatomically interpretable throughout the movement.

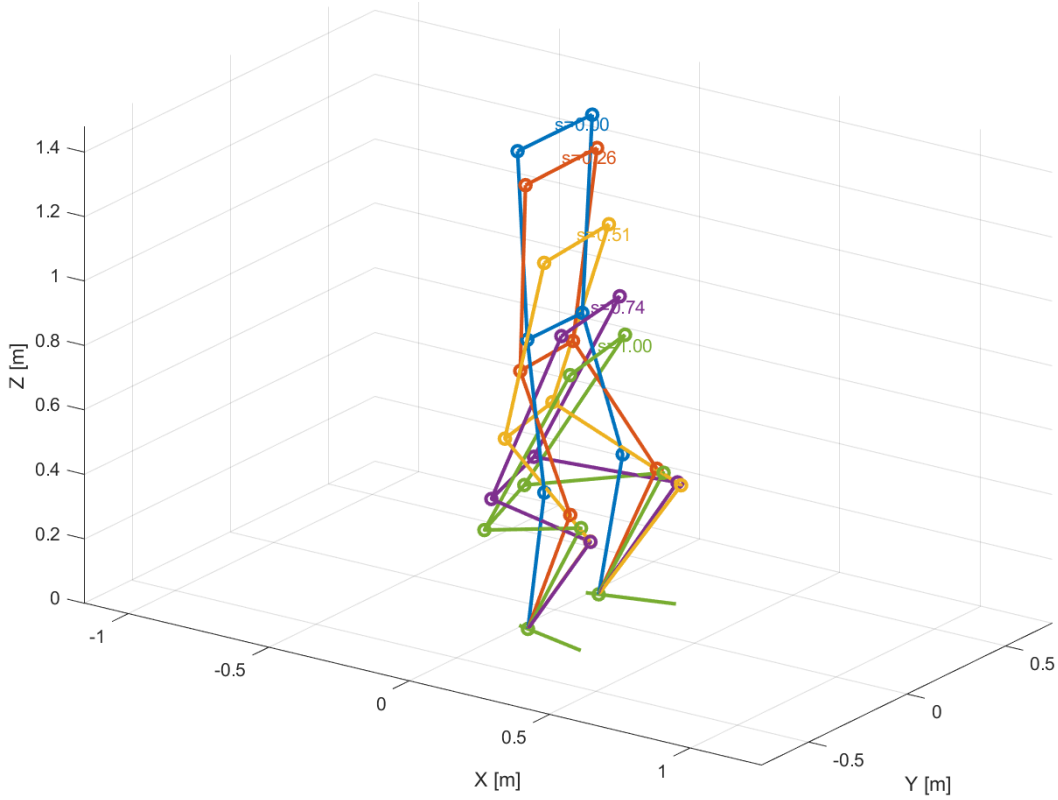

Figure 3. Selected three-dimensional body configurations at representative stages of the squat cycle. Individual configurations correspond to increasing values of the motion parameter s, from initial standing posture to maximum squat depth.

The reconstructed motion remains smooth in the initial stages of the squat and becomes progressively more pronounced with increasing squat depth. This behavior is reflected in the gradual displacement of the pelvis and the increasing torso inclination visible in Figure 3. To quantify these kinematic changes, Figure 4 presents the angular histories of the torso, pelvis, and lower-limb segments. The results show monotonic and continuous evolution of the main angular measures, with similar trends observed for the left and right limbs, which indicates stable and symmetric reconstruction of the motion.

 doi:10.20944/preprints202603.1971.v1

The angular histories shown in Figure 4 indicate that torso pitch and pelvis tilt increase progressively throughout the squat, while the shank and thigh angles evolve smoothly and without abrupt changes. The left and right lower limbs exhibit nearly identical trends, which is consistent with the symmetric formulation adopted in the model. From a kinematic perspective, these results confirm that the generated motion preserves continuity and avoids spurious frame-to-frame oscillations.

An alternative way to assess the reconstructed motion is through the evolution of left–right geometric spacing between corresponding anatomical points. Figure 5 shows the distances between the hip, knee, ankle, and shoulder pairs as functions of the motion parameter s. The nearly constant shoulder, hip, and ankle spacing confirms the preservation of the prescribed segment geometry, while the variation in knee spacing reflects the changing relative configuration of the lower limbs during descent and ascent within the symmetric squat pattern.

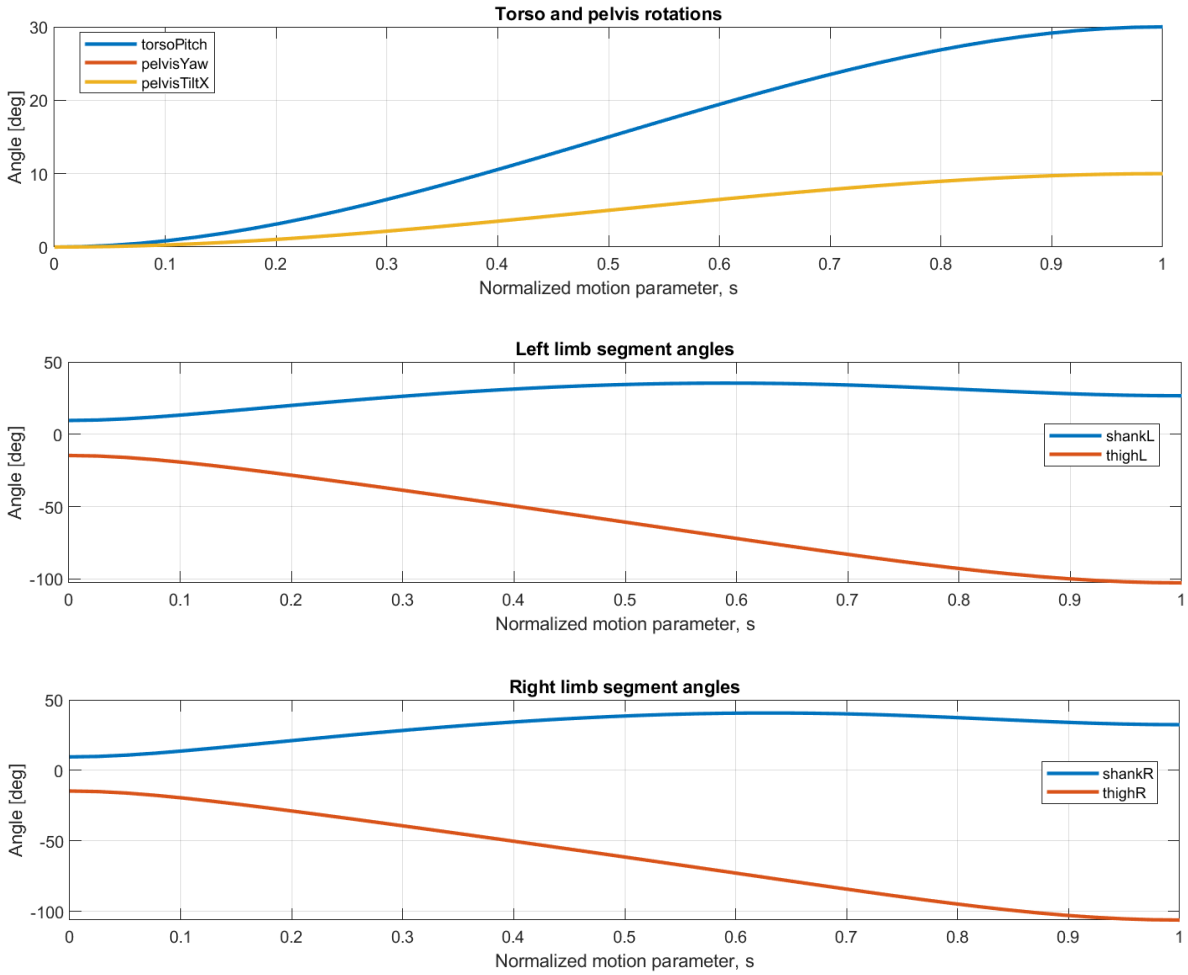

Figure 4. Angular histories of the main body segments: (a) torso pitch and pelvis rotations, (b) left lower limb segment angles (shank and thigh), (c) right lower limb segment angles (shank and thigh). Angles are plotted as functions of the normalized motion parameter s.

The framework is formulated in a way that allows investigation of how squat posture may change when mechanical properties of the joints are modified. In the present study, however, the focus is placed on the kinematic reconstruction of the motion for a representative set of model parameters. Table 1 summarizes the key anthropometric and geometric parameters used in the numerical simulations. These values define the characteristic dimensions of the reconstructed body model and provide the geometric basis for inverse kinematics and posture visualization.

 doi:10.20944/preprints202603.1971.v1

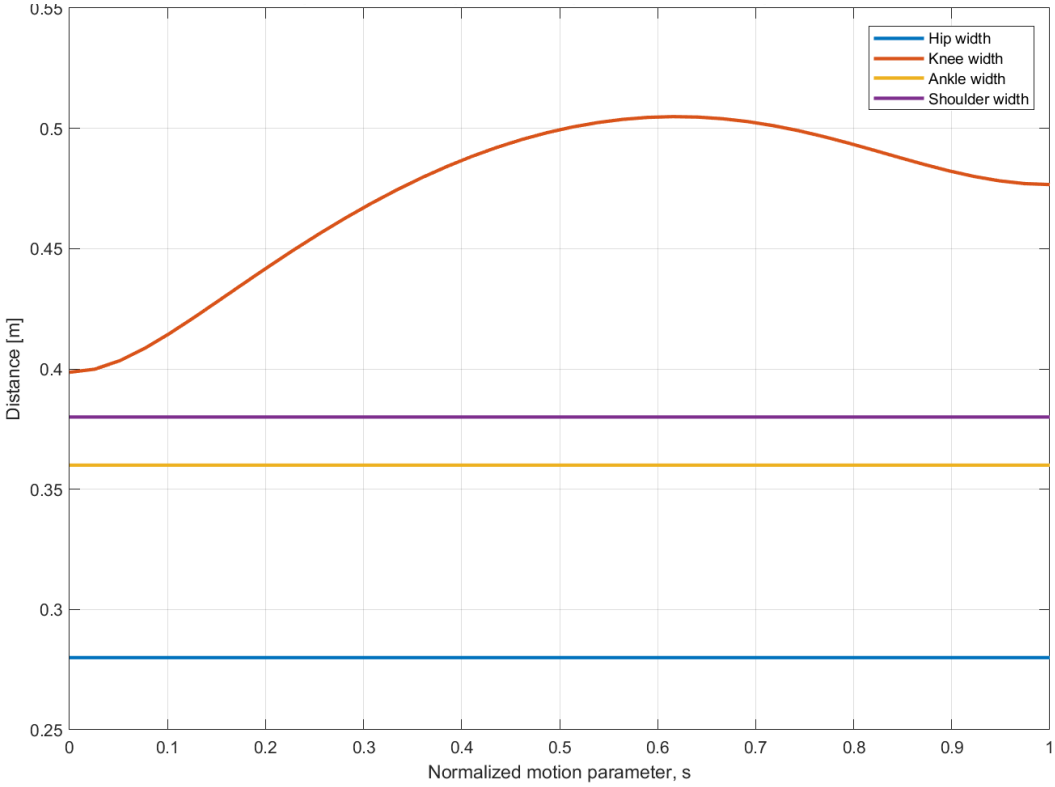

Figure 5. Evolution of left–right spatial relationships between corresponding anatomical points. Distances between hip, knee, ankle, and shoulder joints are shown as functions of the motion parameter s.

Table 1. Anthropometric and geometric parameters used in the numerical simulations.

Parameter	Description	Value
L_s	shank length	0.45 m
L_f	thigh length	0.45 m
L_t	torso length	0.60 m
b_p	pelvis width	0.28 m
b_s	shoulder width	0.38 m

In addition to geometric parameters, the nonlinear joint model requires specification of rotational stiffness and moment capacity for each joint. These values determine the resistance of the system to deviations from the reference motion and therefore play a central role in the mechanical correction process.

To illustrate the evolution of body posture in the sagittal plane, selected motion states are shown in Figure 6 for increasing values of the motion parameter. This representation highlights the progression of pelvis descent, knee flexion, and torso inclination in a compact form and facilitates direct visual comparison between different phases of the squat.

Preprints.org (www.preprints.org) | NOT PEER-REVIEWED | Posted: 25 March 2026 doi:10.20944/preprints202603.1971.v1

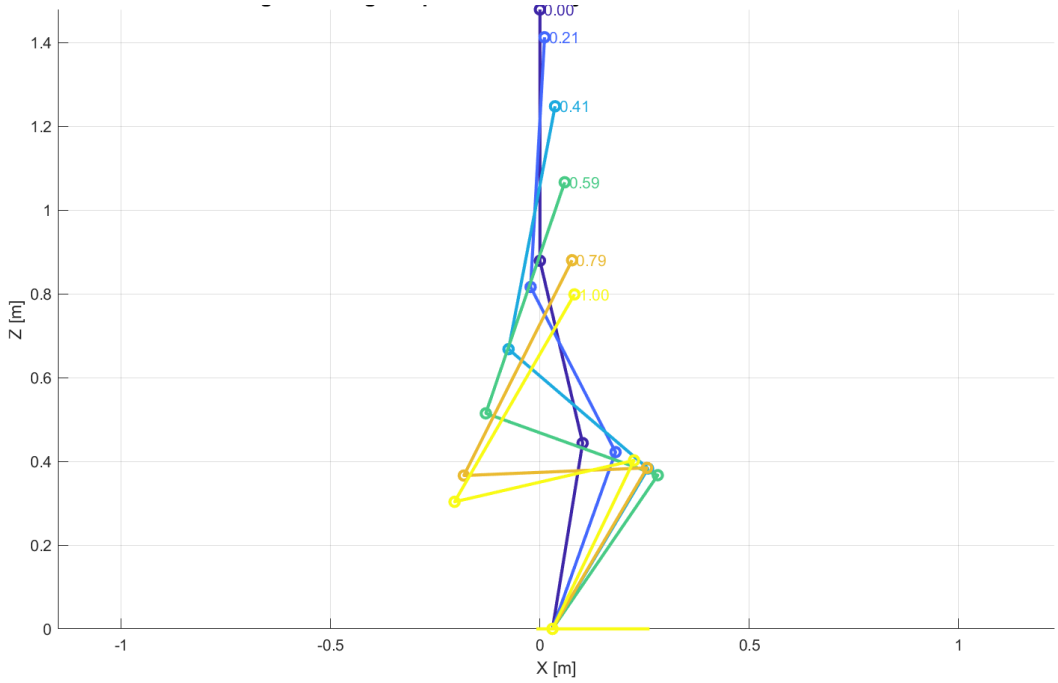

Figure 6. Sagittal-plane body configurations at selected stages of the squat motion: (a) $s \approx 0.0$, (b) $s \approx 0.2$, (c) $s \approx 0.4$, (d) $s \approx 0.6$, (e) $s \approx 0.8$, (f) $s \approx 1.0$. The projection onto the x–$z$plane highlights the evolution of posture, including pelvis displacement, knee flexion, and torso inclination.

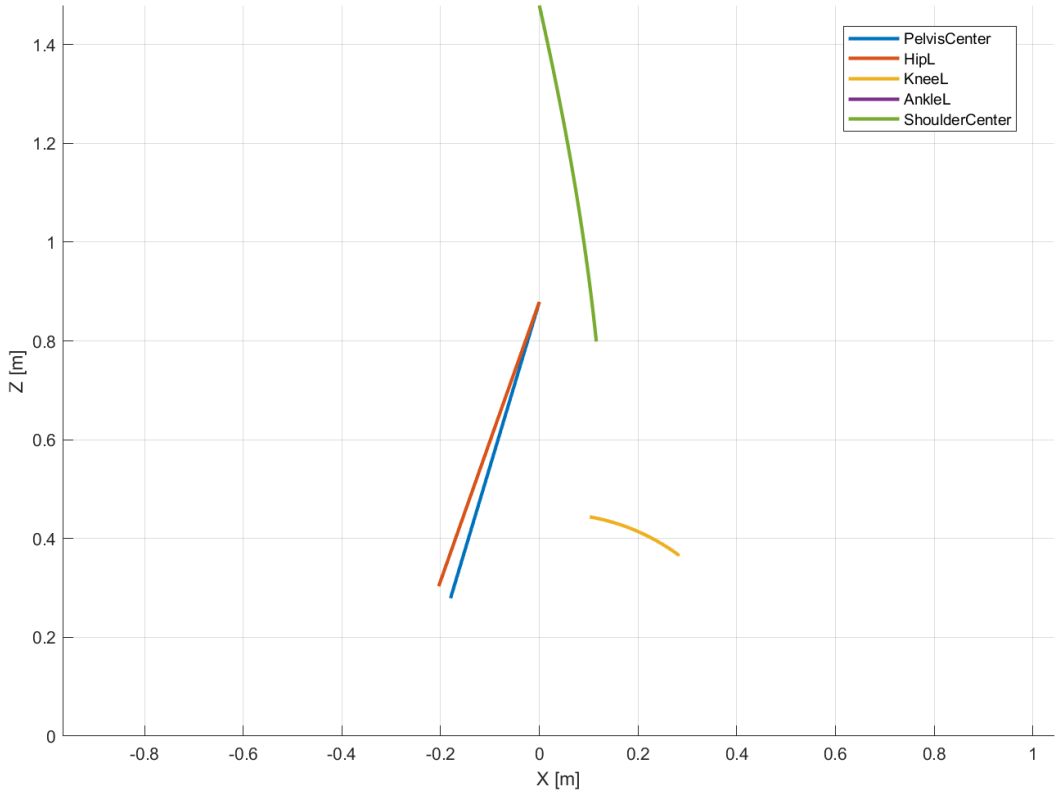

Figure 7. Sagittal trajectories of key anatomical points during the squat motion. The paths of the pelvis center, hip, knee, ankle, and shoulder are shown in the x–z plane.

The sagittal overlays indicate a gradual posterior shift of the pelvis combined with increasing knee flexion and forward rotation of the torso as squat depth increases. This pattern is mechanically plausible and reflects a coordinated reorganization of segment orientation required to maintain the

 doi:10.20944/preprints202603.1971.v1

overall body configuration during deep squatting. The smooth transition between successive poses further supports the numerical stability of the reconstruction procedure.

Finally, the sagittal trajectories of selected anatomical points are summarized in Figure 7. The plotted paths of the pelvis center, hip, knee, ankle, and shoulder provide a compact representation of the overall movement geometry and reveal the relative displacement of the main landmarks during the squat cycle.

The trajectories shown in Figure 7 confirm that the ankle remains effectively fixed, while the pelvis center and hip follow a descending and slightly posterior path, and the shoulder trajectory reflects the progressive forward inclination of the upper body. Taken together, the presented results demonstrate that the proposed framework is capable of reconstructing smooth and mechanically interpretable squat motion while preserving geometric consistency and bilateral symmetry. The adopted visualization set provides a coherent description of the reconstructed kinematics and supports further development toward more advanced mechanically enriched analyses.

4. Discussion

The results presented in Section 3 demonstrate that the proposed computational framework provides a consistent method for reconstructing mechanically admissible squat motion under external loading while accounting for joint moment capacity. The key feature of the method is the integration of a kinematic motion generator with a nonlinear mechanical correction step, allowing the body posture to adapt to strength limitations without explicitly prescribing the final configuration.

One of the main observations is that the reconstructed motion evolves smoothly from the upright posture to the deepest squat position while preserving geometric consistency of the body segments. The progressive posterior displacement of the pelvis and the increase in torso inclination observed in Figures 2, 3, 6, and 7 are consistent with the structure of the optimization problem formulated in Eq. (21), in which the tracking term promotes similarity to the reference trajectory while the mechanical terms penalize unfavorable configurations. As squat depth increases, the solver gradually adjusts the posture rather than producing abrupt changes, which confirms the robustness of the sequential continuation strategy.

The reconstructed kinematic patterns follow trends that are consistent with general biomechanical expectations for squat motion. In particular, the results show gradual pelvis descent, increasing torso inclination, and coordinated evolution of shank and thigh angles, with very similar histories on the left and right sides. This is qualitatively consistent with experimental observations reported in the literature, where squat depth is accompanied by increased trunk inclination and coordinated flexion of the lower-limb segments [2,4,5]. Moreover, the progressive posterior displacement of the pelvis observed in the present model is compatible with descriptions of squat strategies that emphasize “sitting back” and controlled hip-dominant motion [2,8,10].

An important advantage of the proposed formulation is the use of a bounded nonlinear joint model defined in Eq. (15). Unlike purely linear rotational springs, the adopted formulation introduces a natural limit on the achievable joint moments while maintaining smooth behavior suitable for gradient-based optimization. This approach avoids numerical instabilities that may arise when moment limits are imposed through hard constraints and instead allows the solver to approach joint capacity gradually. The resulting moment–rotation relation approximates elastic behavior for small deviations and transitions smoothly toward a saturated response as the moment capacity is approached. From a computational standpoint, this smooth formulation significantly improves the robustness of the optimization procedure.

Another noteworthy aspect of the model is that the bounded nonlinear joint formulation allows posture correction to remain smooth even when the configuration departs progressively from the reference motion. Although the present set of figures focuses on kinematic observables rather than explicit joint moment histories, the reconstructed postures indicate that the framework can accommodate increasing geometric demand without loss of continuity. From a computational

 doi:10.20944/preprints202603.1971.v1

standpoint, this is an important advantage because it enables stable frame-by-frame solution of the squat motion and provides a suitable basis for future extension toward full mechanically enriched output fields.

The proposed method differs conceptually from traditional inverse dynamics approaches commonly used in biomechanics. In inverse dynamics, joint moments are computed from experimentally measured motion, and the resulting loads are interpreted as consequences of the observed movement. In contrast, the present formulation treats joint moment capacity as a constraint that can influence the motion itself. In this sense, the model operates in a complementary direction: instead of asking which joint moments correspond to a given motion, it investigates which motions remain mechanically admissible under specified joint strength limits and external loads. This perspective allows exploration of how movement strategies may adapt to mechanical constraints.

It should be emphasized that the current model intentionally focuses on the dominant mechanical aspects of the squat and therefore adopts several simplifying assumptions. The body segments are treated as rigid links, the feet remain fixed relative to the ground, and muscle forces are not modeled explicitly. Furthermore, the lateral motion of the pelvis is neglected, which effectively constrains the movement to a symmetric configuration. These assumptions reduce the complexity of the model and allow efficient numerical optimization, but they also limit the ability to represent certain aspects of human movement such as asymmetry, balance control, or detailed neuromuscular coordination.

Despite these simplifications, the model provides useful insight into the mechanical interplay between body geometry, joint capacity, and external load. The framework captures the essential mechanism by which posture adjustments can reduce excessive joint moments, thereby maintaining mechanically feasible configurations. This capability suggests that the method could be extended to investigate a variety of human movement scenarios in which joint strength or mechanical limits play a significant role.

Several directions for future work can be identified. First, the model could be extended to include body segment masses and inertial effects, enabling the analysis of dynamic movements rather than quasi-static configurations. Second, introducing explicit contact mechanics between the foot and the ground would allow investigation of balance and center-of-pressure behavior during the squat. Finally, incorporating subject-specific anthropometric parameters and experimentally measured motion trajectories could provide a pathway toward personalized biomechanical analysis.

Overall, the results demonstrate that the proposed optimization-based framework provides a robust and computationally efficient tool for studying mechanically constrained human motion. By explicitly linking posture adaptation with joint moment capacity, the method offers a new perspective on the mechanical determinants of squat technique and provides a foundation for further developments in computational biomechanics.

5. Conclusions

This study presented a computational framework for reconstructing mechanically admissible squat motion under external loading while explicitly accounting for limitations of joint moment capacity. The proposed approach combines a kinematic motion generator, geometric reconstruction of body segments, and a nonlinear optimization procedure that corrects the reference motion according to joint mechanical constraints and external forces.

The human body was represented as a multi-segment rigid system consisting of the feet, shanks, thighs, pelvis, and torso. Joint behavior was modeled using nonlinear rotational elements with bounded moment capacity, enabling a smooth transition from elastic response to a saturated moment regime as joint limits are approached. The resulting formulation allowed the mechanically corrected posture to emerge from the balance between trajectory tracking, joint resistance, and gravitational loading.

The numerical results demonstrated that the proposed method can successfully reconstruct squat motion while maintaining compatibility with geometric and kinematic constraints. The

 doi:10.20944/preprints202603.1971.v1

framework produced smooth evolution of pelvis position, torso inclination, and lower-limb segment angles throughout the squat cycle. The reconstructed body configurations, sagittal overlays, and anatomical trajectories confirmed the continuity, symmetry, and interpretability of the generated motion.

From a methodological perspective, the main advantage of the proposed formulation lies in the integration of motion reconstruction and mechanical constraints within a single optimization framework. Unlike conventional inverse dynamics approaches, which compute joint moments from a prescribed motion, the present method allows the motion itself to adapt in response to mechanical limitations. This provides a complementary perspective for analyzing human movement under strength constraints.

Although the current model adopts several simplifying assumptions, including rigid body segments, fixed foot contact, and quasi-static conditions, it captures the essential mechanical mechanisms governing posture adaptation during the squat. These simplifications enable efficient numerical implementation while preserving the ability to analyze the influence of joint moment capacity on movement patterns.

Future work will focus on extending the framework to dynamic motion analysis, incorporating subject-specific anthropometric data, and introducing more detailed representations of ground contact and musculoskeletal actuation. Such developments may broaden the applicability of the method to a wider range of human movement analyses and support the use of computational models in biomechanics, sports science, and human-centered engineering design.

Author Contributions: Conceptualization, K.N.; methodology, K.N., A.S.-G. and T.G.; software, K.N. and T.G.; validation, K.N., A.S.-G., A.C. and T.G.; formal analysis, K.N.; investigation, K.N.; resources, K.N. and A.C.; data curation, K.N. and A.C.; writing—original draft preparation, K.N.; writing—review and editing, A.S.-G., A.C. and T.G.; visualization, K.N. and T.G.; supervision, A.S.-G. and T.G.; project administration, A.S.-G. and T.G.; funding acquisition, A.S.-G. and A.C. All authors have read and agreed to the published version of the manuscript.

Funding: This research received no external funding.

Institutional Review Board Statement: Not applicable.

Informed Consent Statement: Not applicable.

Data Availability Statement: The original contributions presented in this study are included in the article. Further inquiries can be directed to the corresponding author.

Conflicts of Interest: The authors declare no conflicts of interest.

Appendix A

This appendix summarizes the numerical procedure used to compute the mechanically admissible squat motion described in this study. The algorithm integrates the following components:

- generation of a reference squat trajectory,
- geometric reconstruction of the body segments,
- inverse kinematics of the lower limbs,
- evaluation of nonlinear joint moments,
- frame-by-frame mechanical correction using constrained optimization,
- progressive update of joint mechanical properties when moment limits are exceeded.

The algorithm operates sequentially along the squat trajectory, which is discretized into a series of frames.

Appendix A.1. Main Computational Workflow

 doi:10.20944/preprints202603.1971.v1

INPUT
Anthropometric parameters

- L_shank, L_thigh, L_torso
- pelvis_width
- shoulder_width

Initial configuration

- ankle positions A_L, A_R
- initial pelvis coordinates

Motion parameters

- pelvis_drop_max
- pelvis_backshift_max
- pelvis_yaw_max
- pelvis_tilt_max
- torso_pitch_max
- number of frames N

Mechanical parameters

- barbell mass m_b
- gravitational acceleration g
- joint stiffness k_j
- joint moment capacities $M_{y,j}$
- tracking stiffness matrix K_{track}

OUTPUT

- reference trajectory $q_{\text{ref}}(n)$
- corrected trajectory $q_{\text{corr}}(n)$
- reconstructed poses $\text{pose}_{\text{corr}}(n)$
- joint moments $M_j(n)$
- joint utilization ratios

PROCEDURE

Initialize anthropometric parameters and mechanical parameters.

1. Compute a feasible initial pelvis height from the lower limb geometry.
2. Generate the reference squat trajectory $q_{\text{ref}}(n)$ for all frames.
3. Initialize joint state variables (elastic stiffness, yielding flags).
4. For each frame $n = 1 \ldots N$ perform:

a. Set current reference configuration $q_{\text{ref}} = q_{\text{ref}}(n)$

b. Select initial guess for optimization

i. first frame → q_{ref}

ii. otherwise → previous corrected solution

c. Solve the mechanical correction problem

d. Reconstruct the corrected body pose

 doi:10.20944/preprints202603.1971.v1

e. Compute joint angles and joint moments

f. Evaluate joint utilization ratios

g. Update joint stiffness if yielding condition is reached

5. Store all results for post-processing.

Algorithm A2. Generation of Reference Squat Trajectory

INPUT

- initial pelvis position (x_{p0}, z_{p0})
- motion amplitudes $(\Delta x_p, \Delta z_p)$
- maximum pelvis rotations
- maximum torso rotation
- number of frames N

PROCEDURE

For each frame $n = 1 \ldots N$

Compute normalized motion parameter

$s = (n-1)/(N-1)$.

Evaluate motion profile function

$f = 3s^2 - 2s^3$.

Compute pelvis coordinates

$x_p(n) = x_{p0} - \Delta x_p \cdot f,$

$z_p(n) = z_{p0} - \Delta z_p \cdot f.$

Compute pelvis rotations

$\psi_p(n) = \psi_{max} \cdot f.$

$\varphi_p(n) = \varphi_{max} \cdot f.$

Compute torso rotation

$\theta_t(n) = \theta_{t,\max} \cdot f.$

Assemble generalized coordinate vector

$q_{\text{ref}}(n) = [x_p(n), z_p(n), \psi_p(n), \varphi_p(n), \theta_t(n)].$

OUTPUT

Reference trajectory $q_{\text{ref}}(n)$

Algorithm A3. Reconstruction of Body Geometry

INPUT

- generalized coordinates q
- anthropometric parameters
- fixed ankle positions

PROCEDURE

Extract coordinates

$x_p, z_p, \psi_p, \varphi_p, \theta_t.$

 doi:10.20944/preprints202603.1971.v1

Compute pelvis center

$p_p = (x_p, 0, z_p)$.

Compute pelvis rotation matrix

$R_p = R_z(\psi_p) \cdot R_x(\varphi_p)$.

Determine pelvis transverse direction

$e_y = R_p \cdot (0,1,0)$.

Compute hip positions

$p_{HL} = p_p + (\text{pelvis\_width}/2) \cdot e_y$,

$p_{HR} = p_p - (\text{pelvis\_width}/2) \cdot e_y$.

Use fixed ankle coordinates

$p_{AL} = A_L$,

$p_{AR} = A_R$.

Reconstruct torso orientation

Compute shoulder center

$p_S = p_p + L_{\text{torso}} \cdot \text{direction\_torso}$.

Compute left and right shoulder positions

Determine toe and heel points from ankle and foot orientation

OUTPUT

Complete body pose

Algorithm A4. Inverse Kinematics of One Leg

INPUT

- hip position p_H
- ankle position p_A
- thigh length L_{thigh}
- shank length L_{shank}

PROCEDURE

Compute hip coordinates relative to ankle

x_H = projection along sagittal direction

z_H = vertical coordinate difference

Compute hip-ankle distance

$d = \sqrt{(x_H^2 + z_H^2)}$.

Check geometric feasibility

$|L_{\text{thigh}} - L_{\text{shank}}| \le d \le L_{\text{thigh}} + L_{\text{shank}}$.

Solve intersection of two circles

circle 1: center at ankle, radius L_{shank}

circle 2: center at hip, radius L_{thigh}

 doi:10.20944/preprints202603.1971.v1

Select physically consistent knee solution

Compute shank and thigh angles

OUTPUT

- knee coordinates
- thigh angle
- shank angle

Algorithm A5. Computation of Joint Moments

INPUT

- current joint angles
- reference joint angles
- stiffness parameters
- moment capacities

PROCEDURE

For each joint j

Compute angular deviation

$$\Delta\theta_j = \theta_j - \theta_j^{\mathrm{ref}}.$$

Compute nonlinear joint moment

$$M_j = M_{y,j} \cdot \tanh\big((k_j \cdot \Delta\theta_j)/M_{y,j}\big).$$

Compute utilization ratio

$$u_j = |M_j|/M_{y,j}.$$

OUTPUT

Joint moments and utilization ratios

Algorithm A6. Mechanical Correction in One Frame

INPUT

- reference coordinates q_{ref}
- previous corrected coordinates
- anthropometric parameters
- mechanical parameters

PROCEDURE

Select initial guess

Define objective function

$$\Pi(q) = \Pi_{\mathrm{track}} + \Pi_{\mathrm{joint}} + \Pi_{\mathrm{ext}}.$$

Define geometric constraints

- lower limb reachability

 doi:10.20944/preprints202603.1971.v1

- coordinate bounds

Solve constrained optimization problem

$$q_{corr} = arg\ \min_{q}\ \Pi(q).$$

Reconstruct corrected body configuration

Compute joint angles and moments

OUTPUT

Corrected coordinates q_{corr} and joint state

Algorithm A7. Joint Yielding Update

INPUT

- current joint moments
- joint capacities
- yield threshold

PROCEDURE

For each joint j

if $|M_j| \geq \eta_y \cdot M_{y,j}$, then

* mark joint as yielded

* reduce active stiffness

OUTPUT

Updated joint stiffness parameters

Algorithm A8. Sequential Solution Along the Motion

INPUT

Reference trajectory $q_{\mathrm{ref}}(n)$

PROCEDURE

for $n = 1 \ldots N$

Perform mechanical correction for frame n

Update joint moments and stiffness

Store corrected configuration

Use current solution as initial guess for next frame

OUTPUT

- corrected motion trajectory
- joint moment histories
- joint utilization maps

Remark: The presented algorithm describes the computational procedure used to obtain the results reported in this study. The modular structure of the framework allows straightforward extensions, such as the inclusion of dynamic effects, subject-specific anthropometric data, or more advanced joint constitutive models.

 doi:10.20944/preprints202603.1971.v1

References

2. Chandler, T.J.; Stone, M.H. The squat exercise in athletic conditioning: A position statement and review of the literature. *Strength Cond. J.* 1991, **13**, 51–60.
3. Swinton, P.A.; Lloyd, R.; Keogh, J.W.L.; Agouris, I.; Stewart, A.D. A biomechanical comparison of the traditional squat, powerlifting squat, and box squat. *J. Strength Cond. Res.* 2012, **26**, 1805–1816.
4. McLaughlin, T.M.; Dillman, C.J.; Lardner, T.J. A kinematic model of performance in the parallel squat by champion powerlifters. *Med. Sci. Sports Exerc.* 1977, **9**, 128–133.
5. Escamilla, R.F.; Fleisig, G.S.; Lowry, T.M.; Barrentine, S.W.; Andrews, J.R. A three-dimensional biomechanical analysis of the squat during varying stance widths. *Med. Sci. Sports Exerc.* 2001, **33**, 984–998.
6. Schoenfeld, B.J. Squatting kinematics and kinetics and their application to exercise performance. *J. Strength Cond. Res.* 2010, **24**, 3497–3506.
7. McCaw, S.T.; Melrose, D.R. Stance width and bar load effects on leg muscle activity during the parallel squat. *Med. Sci. Sports Exerc.* 1999, **31**, 428–436.
8. Paoli, A.; Marcolin, G.; Petrone, N. The effect of stance width on the electromyographical activity of eight superficial thigh muscles during back squat with different loads. *J. Strength Cond. Res.* 2009, **23**, 246–250.
9. Chiu, L.Z.F.; Heiler, J.; Sorenson, S.C. Sitting back in the squat. *Strength Cond. J.* 2009, **31**, 25–27.
10. Stone, M.H.; Hornsby, W.G.; Mizuguchi, S.; Sato, K.; Gahreman, D.; Duca, M.; Carroll, K.M.; Ramsey, M.W.; Stone, M.E.; Pierce, K.C.; et al. The Use of Free Weight Squats in Sports: A Narrative Review—Terminology and Biomechanics. Appl. Sci. 2024, 14, 1977. https://doi.org/10.3390/app14051977
11. Fry, A.C.; Smith, C.; Schilling, B.K. Effect of knee position on hip and knee torques during the barbell squat. *J. Strength Cond. Res.* 2003, **17**, 629–633.
12. Hales, M.E.; Johnson, B.F.; Johnson, J.T. Kinematic analysis of the powerlifting style squat and the conventional deadlift during competition: Is there a cross-over effect between lifts? *J. Strength Cond. Res.* 2009, **23**, 2574–2580.
13. Escamilla, R.F.; Fleisig, G.S.; Zheng, N.; Lander, J.E.; Barrentine, S.W.; Andrews, J.R.; Bergemann, B.W.; Moorman, C.T. Effects of technique variations on knee biomechanics during the squat and leg press. *Med. Sci. Sports Exerc.* 2001, **33**, 1552–1566.
14. McBride, J.M.; Skinner, J.W.; Schafer, P.C.; Haines, T.L.; Kirby, T.J. Comparison of kinetic variables and muscle activity during a squat vs. a box squat. *J. Strength Cond. Res.* 2010, **24**, 3195–3199.
15. Wretenberg, P.; Feng, Y.; Arborelius, U.P. High- and low-bar squatting techniques during weight-training. *Med. Sci. Sports Exerc.* 1996, **28**, 218–224.
16. Pereira, G.R.; Leporace, G.; Chagas, D.V.; Furtado, L.F.L.; Praxedes, J.; Batista, L.A. Influence of hip external rotation on hip adductor and rectus femoris myoelectric activity during a dynamic parallel squat. *J. Strength Cond. Res.* 2010, **24**, 2749–2754.
17. Signorile, J.F.; Kwiatkowski, K.; Caruso, J.F.; Robertson, B. Effect of foot position on the electromyographical activity of the superficial quadriceps muscles during the parallel squat and knee extension. *J. Strength Cond. Res.* 1995, **9**, 182–187.
18. Decker, M.; Krong, J.; Peterson, D.; Anstett, T.; Torry, M.; Giphart, E.; Shelburne, K.; Philippon, M. Deep hip muscle activation during a squat exercise. In *Proceedings of the American Society of Biomechanics*; PA, USA, 2009.
19. Ireland, M.L. The female ACL: Why is it more prone to injury? *Orthop. Clin. North Am.* 2002, **33**, 637–651.
20. Leetun, D.T.; Ireland, M.L.; Willson, J.D.; Ballantyne, B.T.; Davis, I.M. Core stability measures as risk factors for lower extremity injury in athletes. *Med. Sci. Sports Exerc.* 2004, **36**, 926–934.
21. Kadaba, M.P.; Ramakrishnan, H.K.; Wooten, M.E. Measurement of lower extremity kinematics during level walking. *J. Orthop. Res.* 1990, **8**, 383–392.
22. Gutierrez-Farewik, E.M.; Bartonek, A.; Saraste, H. Comparison and evaluation of two common methods to measure center of mass displacement in three dimensions during gait. *Hum. Mov. Sci.* 2006, **25**, 238–256.
23. Kawamori, N.; Rossi, S.J.; Justice, B.D.; Haff, E.E.; Pistilli, E.E.; O'Bryant, H.S.; Stone, M.H.; Haff, G.G. Peak force and rate of force development during isometric and dynamic mid-thigh clean pulls performed at various intensities. *J. Strength Cond. Res.* 2006, **20**, 483–491.

 doi:10.20944/preprints202603.1971.v1

24. Cormie, P.; McCaulley, G.O.; Triplett, N.T.; McBride, J.M. Optimal loading for maximal power output during lower-body resistance exercises. *Med. Sci. Sports Exerc.* 2007, **39**, 340–349.
25. Zink, A.J.; Perry, A.C.; Robertson, B.L.; Roach, K.E.; Signorile, J.F. Peak power, ground reaction forces, and velocity during the squat exercise performed at different loads. *J. Strength Cond. Res.* 2006, **20**, 658–664.
26. Cronin, J.; Sleivert, G. Challenges in understanding the influence of maximal power training on improving athletic performance. *Sports Med.* 2005, **35**, 213–234.
27. Wilson, G.J.; Murphy, A.J.; Pryor, J.F. Musculotendinous stiffness: Its relationship to eccentric, isometric, and concentric performance. *J. Appl. Physiol.* 1994, **76**, 2714–2719.
28. Brown, L.E.; Shepard, G.; Sjostrom, T. Performance box squats. *Strength Cond. J.* 2003, **25**, 22–23.
29. Wu, H.; Lee, S.; Kao, J.; Wang, S. Three-dimensional kinetic analysis of lower limbs in barbell squat. In *Proceedings of the 37th Annual Northeast Bioengineering Conference*; Rochester, NY, USA, 2011.
30. Swinton, P.A.; Lloyd, R.; Agouris, I.; Stewart, A. Contemporary training practices in elite British powerlifters: Survey results from an international competition. *J. Strength Cond. Res.* 2009, **23**, 380–384.
31. American College of Sports Medicine. Progression models in resistance training for healthy adults. *Med. Sci. Sports Exerc.* 2009, **41**, 687–708.